Deciphering Allosteric Mechanisms in KRAS Activation: Insights from GTP-Induced Conformational Dynamics and Intramolecular Interaction Network Reorganization

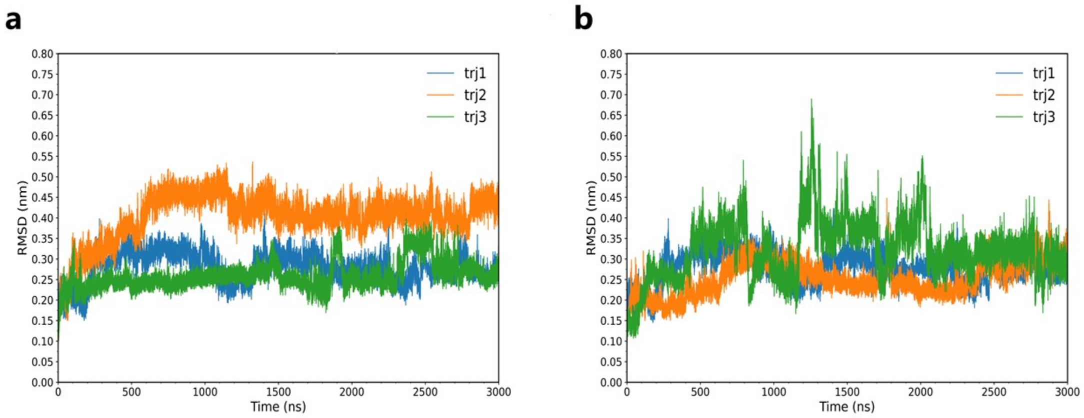

Figure S1. The root mean square deviation (RMSD) of the three trajectories in the GDP-bound state and GTP-bound state. (a) GDP-bound , (b) GTP-bound.

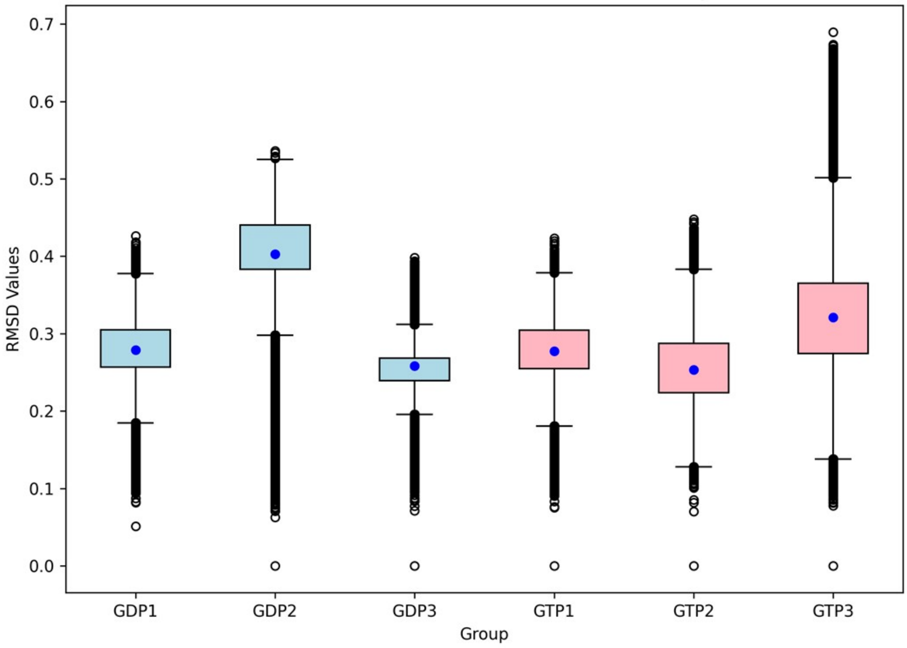

Figure S2. The box plot of the root mean square deviation (RMSD) for the three trajectories in both the GDP-bound state and the GTP-bound state. The blue color represents the GDP-bound state, while the pink color represents the GTP-bound state. The dark blue dot represents the average value.

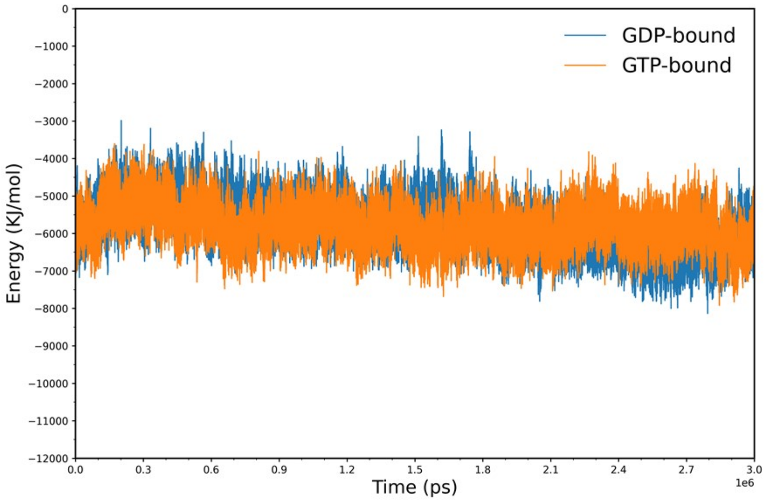

Figure S3. Potential energy as a function of time for GDP-bound (blue) and GTP-bound (orange) states. The GDP-bound system displayed higher variability with energy values generally lower than -4000 kJ/mol, while the GTP-bound system maintained a slightly more stable energy profile near -7000 kJ/mol.

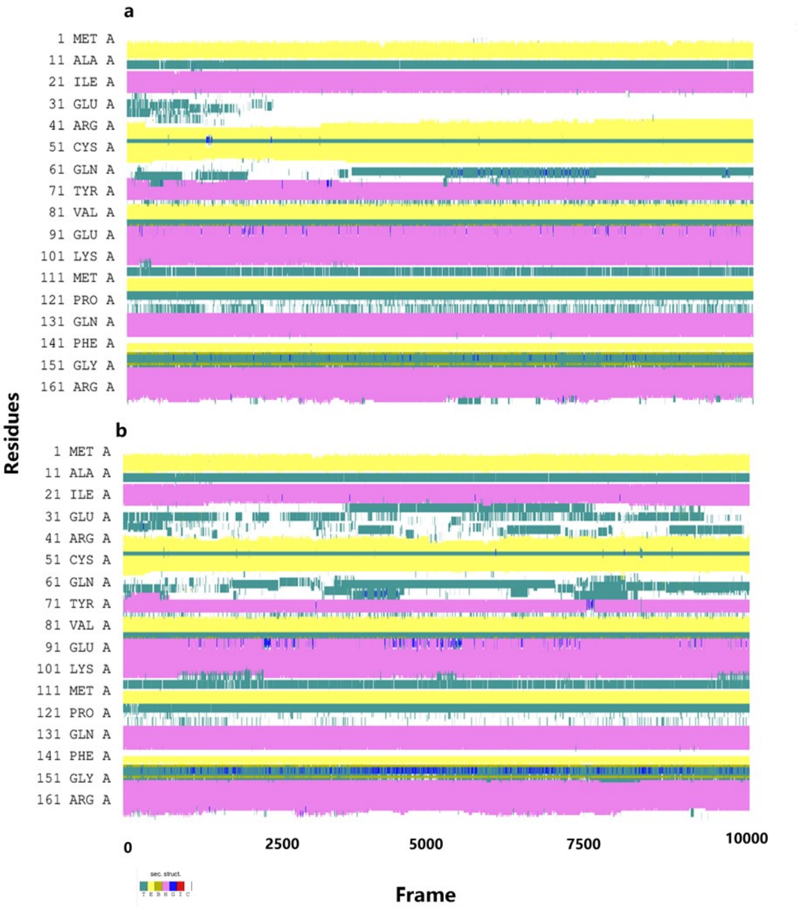

Figure S4. 10000 frames of the change of the secondary junction over time at different temperatures were captured. (a) RAS-GDP-bound . (b) RAS-GTP-bound. Among them, the corner is represented in green, the α-helix is represented in purple, the 3/10-helix is represented in dark blue, the pai-helix is represented in red, the β-pleated sheet is represented in yellow, the β-bridge is represented in yellow-green, and the random coil is represented in white.

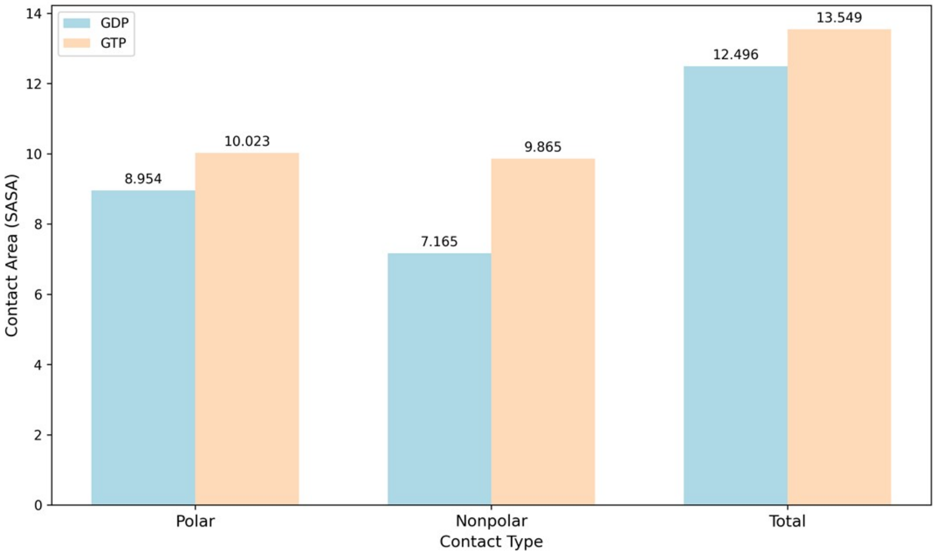

Figure S5. Statistical distribution of polar, nonpolar, and total contact areas for GDP–bound and GTP-bound molecules.

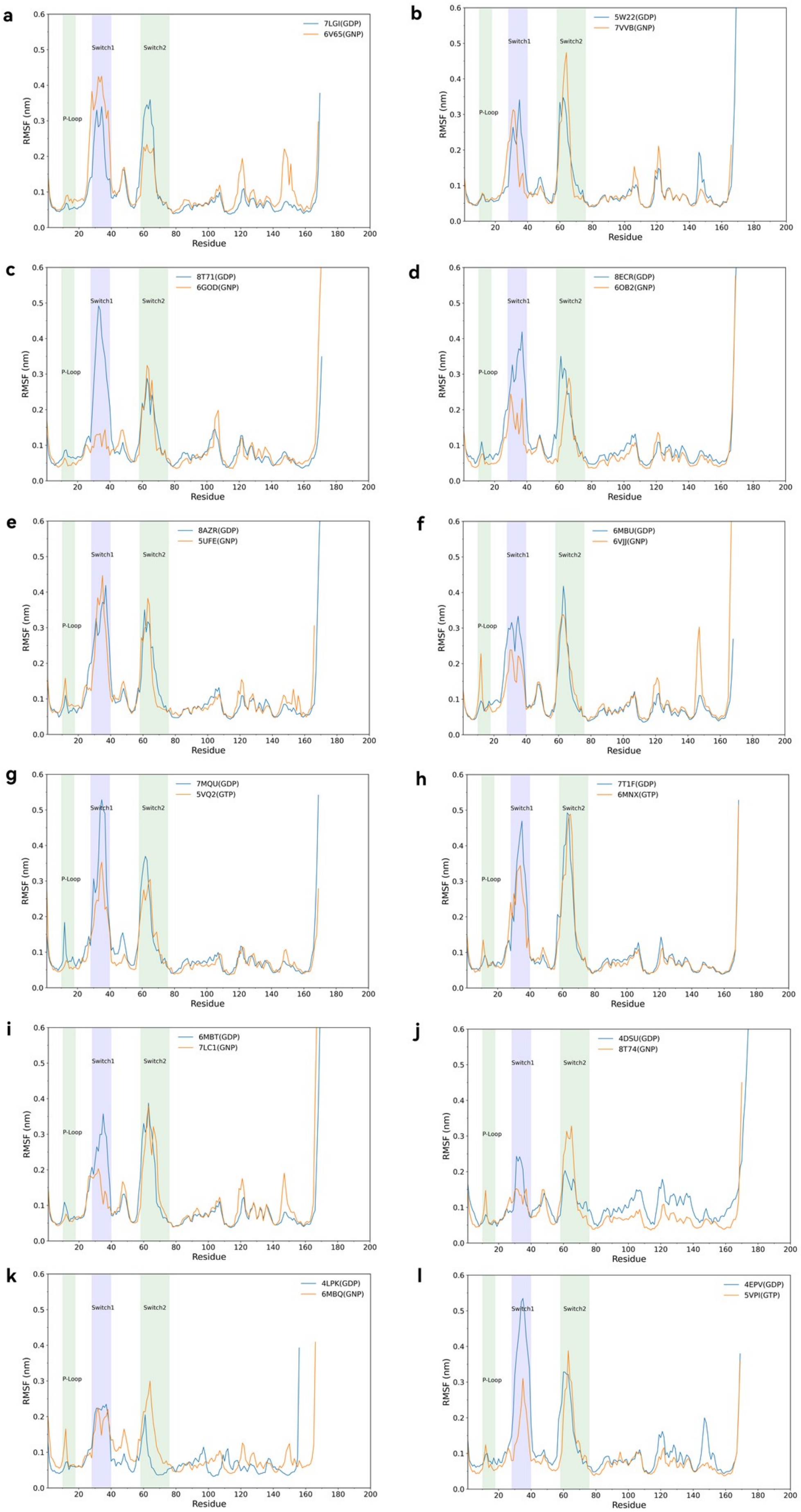
a
7LGI(GDP)
6V65(GNP)
b
5W22(GDP)
7VVB(GNP)
c
8T71(GDP)
6GOD(GNP)
d
8ECR(GDP)
6OB2(GNP)
e
8AZR(GDP)
5UFE(GNP)
f
6MBU(GDP)
6VJJ(GNP)
g
7MQU(GDP)
5VQ2(GTP)
h
7T1F(GDP)
6MNX(GTP)
i
6MBT(GDP)
7LC1(GNP)
j
4DSU(GDP)
8T74(GNP)
k
4LPK(GDP)
6MBQ(GNP)
l
4EPV(GDP)
5VPI(GTP)
P-Loop
Switch1
Switch2
RMSF (nm)
Residue
0.0
0.1
0.2
0.3
0.4
0.5
0.6
20
40
60
80
100
120
140
160
180
200

Figure S6. Root mean square fluctuation (RMSF) values of 24 crystal structures in both the KRAS-GDP bound state and the GTP/GNP bound state .

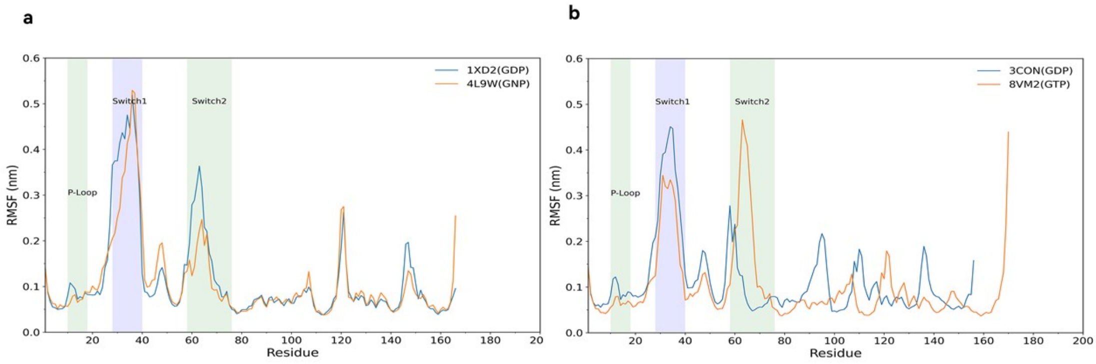

Figure S7. The Root Mean Square Fluctuation(RMSF) diagram of HRAS and NRAS binding to GDP and GTP/GNP. (a) The FMSF diagram of HRAS, and the conformational flexibility of HRAS binding to GDP and GNP is roughly the same. (b) The RMSF diagram of NRAS. The region of GTP-binding state switch 2 has a higher conformational flexibility, while other regions have slightly lower conformational flexibility compared to GDP-binding.

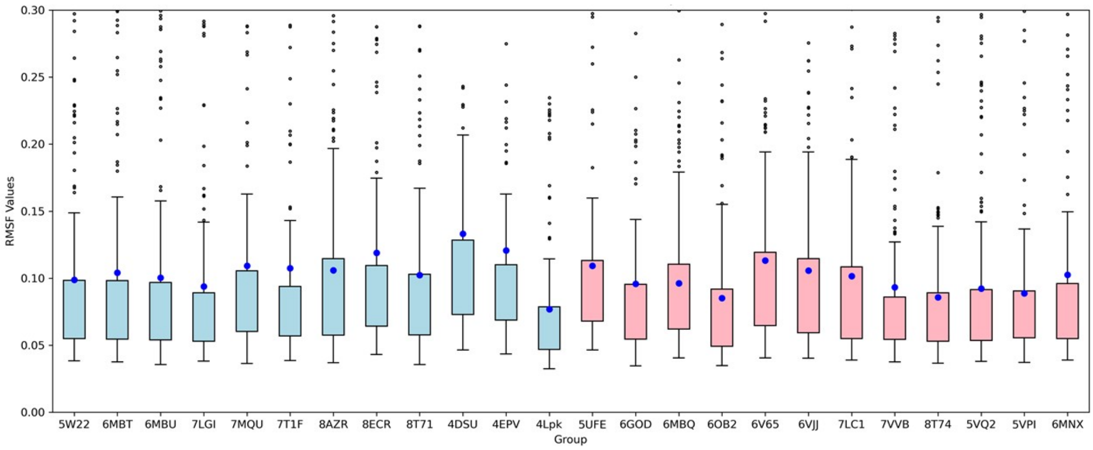

Figure S8. Box plot of root mean square fluctuation (RMSF) values for 24 crystal structures in the KRAS-GDP bound state and the GTP/GNP bound state. Among them, blue represents GDP results, and gray represents GTP/GNP results. The dark blue dot represents the average value.

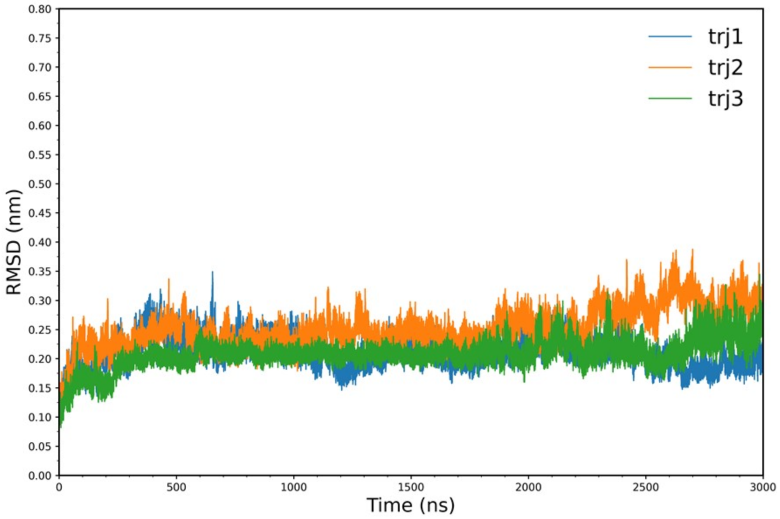

Figure S9. The root mean square deviation (RMSD) of the protein without GDP-bound and GTP-bound states.

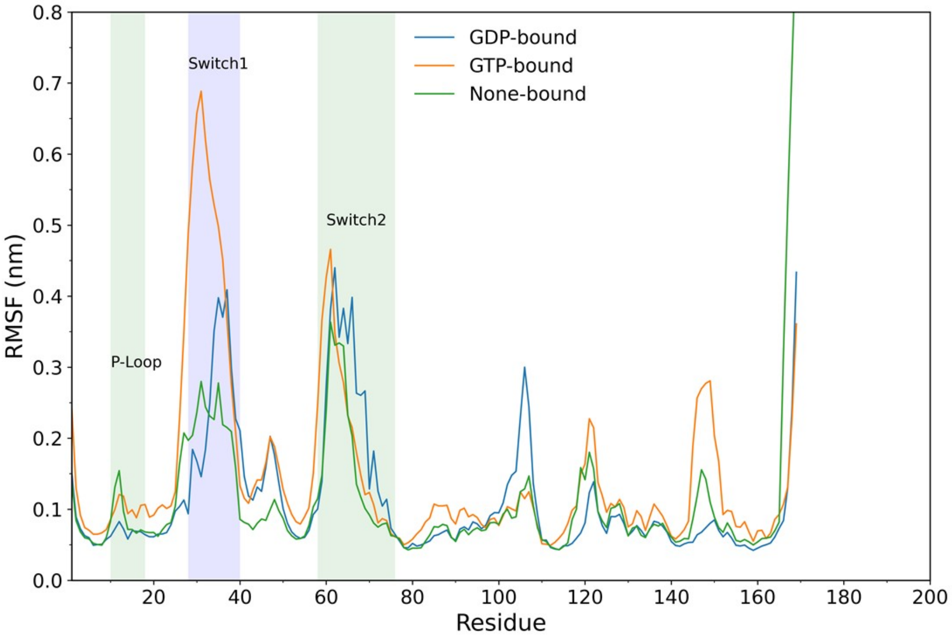

Figure S10. The Root Mean Square Fluctuation(RMSF) diagram of the GDP-bound，GTP-bound and protein without GDP-bound and GTP-bound states.

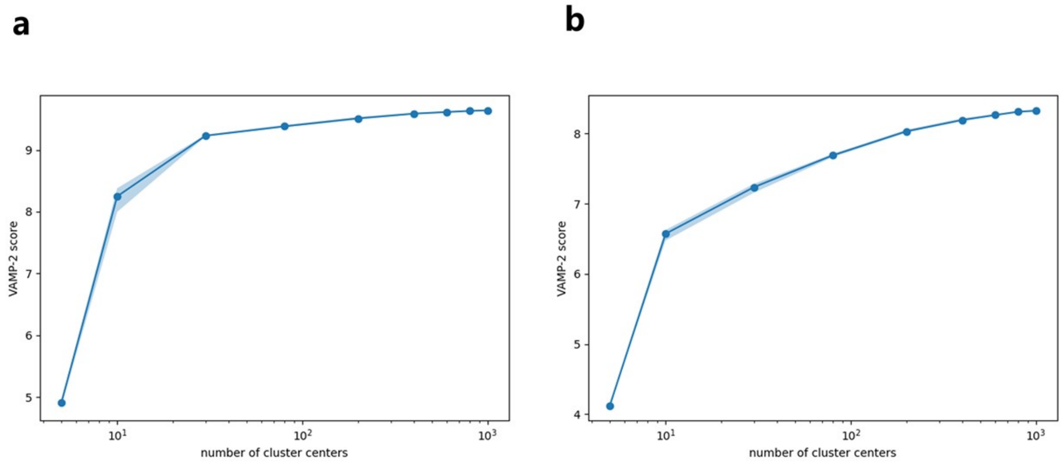

Figure S11. VAMP-2 score for different numbers of cluster centers. (a) GDP-bound， (b) GTP-bound.

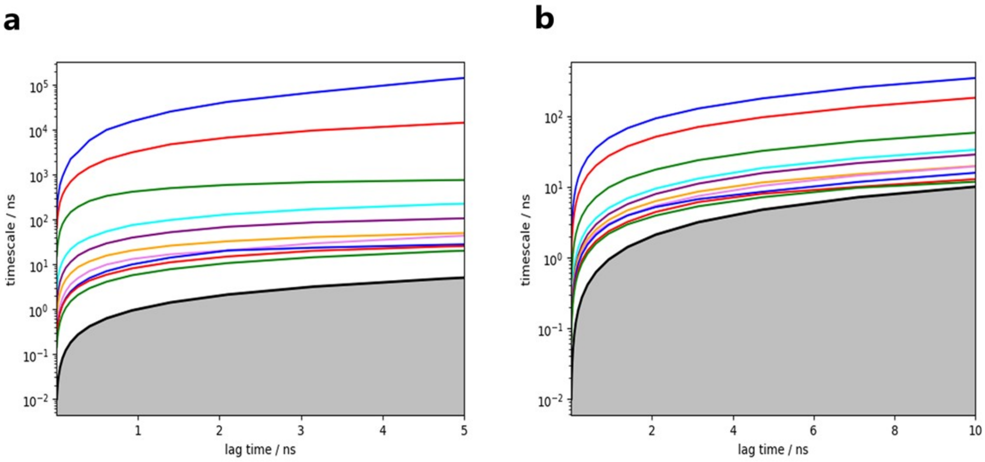

Figure S12. Implied timescales. (a) GDP-bound， (b) GTP-bound.

Table S1. The distribution of the four states of the protein without GDP-bound and GTP-bound, as well as the mean first passage time between each state.

State(distribution)	1 (11.69%)	2 (20.57%)	3 (31.12%)	4 (36.61%)
1 (11.69%)	0.00ns	12.94ns	16.22ns	26.63ns
2 (20.57%)	4.00ns	0.00ns	22.22ns	32.73ns

3	(31.12%)	13.83ns	37.12ns	0.00ns	31.65ns
4	(36.61%)	22.26ns	46.82ns	28.55ns	0.00ns

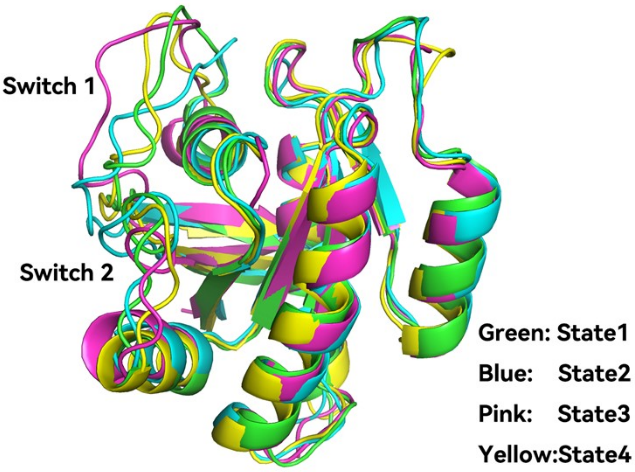

Figure S13. The KRAS protein substates without ligand binding all exhibit four transition states that are in a non-activated state.

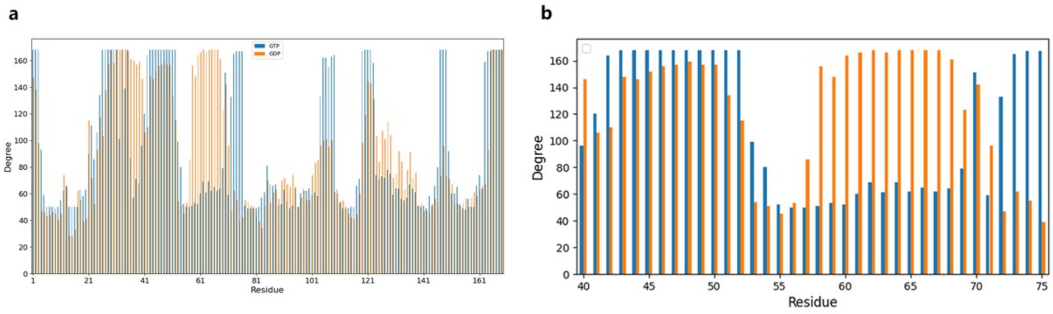

Figure S14. Degree distribution by residue, The GTP-bound (blue) state exhibits a shorter average path length (1.4456 vs. 1.4602), higher average degree (93.1361 vs. 90.6864), and significantly greater average interaction weight (64.9822 vs. 31.4900). (a) The distribution of values for all residues. (b) Highlights the distribution of values for residues 40-75.

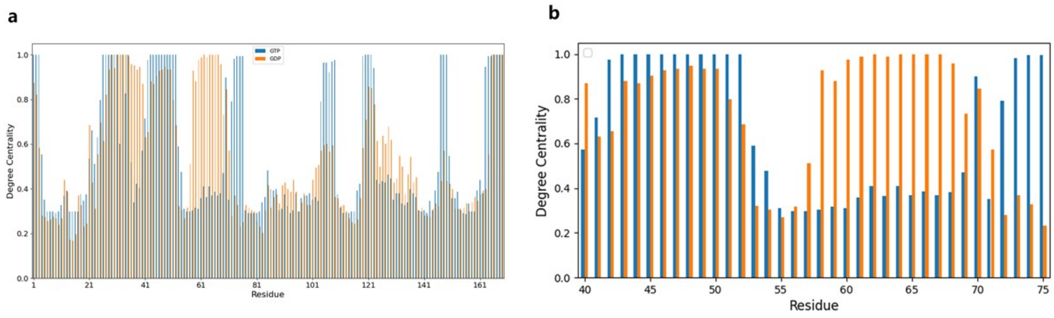

Figure S15. Degree centrality distribution by residue, centrality measures such as average degree centrality (0.5544 vs. 0.5398). (a) The distribution of values for all residues. (b) Highlights the distribution of values for residues 40-75.

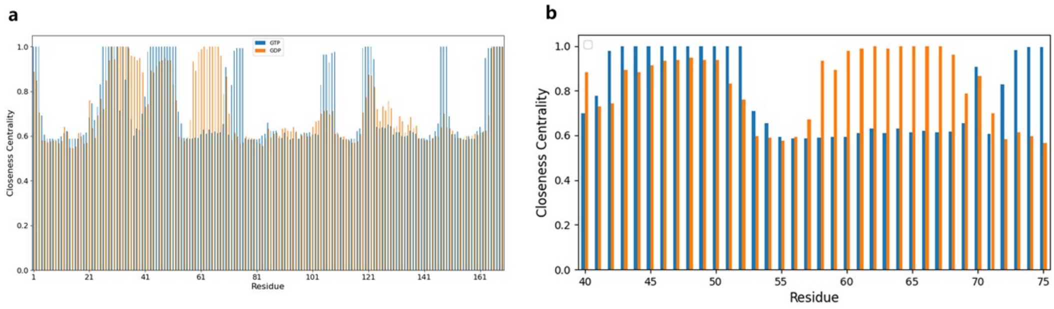

Figure S16. Closeness centrality distribution by residue , GTP(blue) vs GDP(orange) is (0.7255 vs. 0.7124). (a) The distribution of values for all residues. (b) Highlights the distribution of values for residues 40-75.

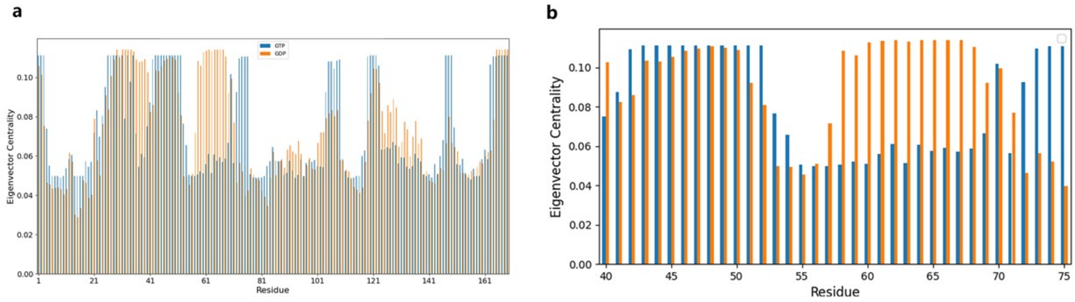

Figure S17. Eigenvector centrality distribution by residue , GTP(blue) vs GDP(orange) is (0.0728 vs. 0.0725). (a) The distribution of values for all residues. (b) Highlights the distribution of values for residues 40-75.

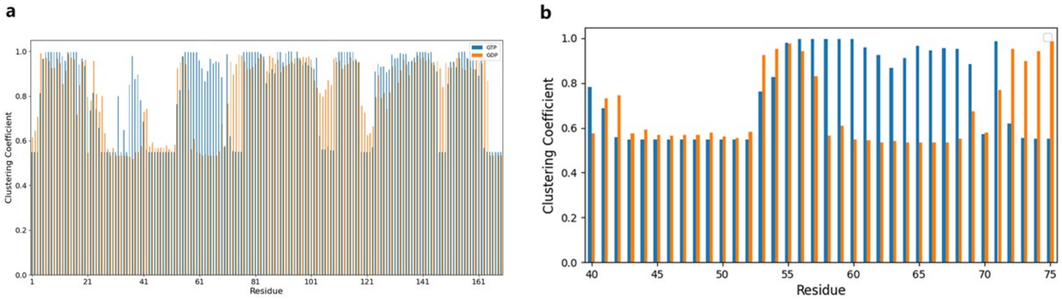

Figure S18. Clustering coefficient distribution by residue , GTP(blue) vs GDP(orange) is (0.8309 vs. 0.8148). (a) The distribution of values for all residues. (b) Highlights the distribution of values for residues 40-75.

Table S2. Path Probabilities to Switch 1 and Switch 2 of GDP-bound State

GDP-bound-sw1		GDP-bound-sw2	
Pathways(resi)	Probability/%	Pathways(resi)	Probability/%
12 - 31	0.1195	13 - 64	0.1396
12 - 32	0.1186	12 - 64	0.1322
17 - 33	0.1157	13 - 65	0.1278
12 - 33	0.1144	12 - 65	0.1134
13 - 31	0.1107	13 - 62	0.1117
17 - 32	0.1095	17 - 64	0.1061
13 - 32	0.1070	12 - 62	0.1037
13 - 33	0.1029	17 - 65	0.0885
17 - 31	0.1016	17 - 62	0.0769

Table S3. Path Probabilities to Switch 1 and Switch 2 of GTP-bound State

GTP-bound-sw1		GTP-bound-sw2	
Pathways(resi)	Probability/%	Pathways(resi)	Probability/%
11-69-28	0.1833	11-107-74	0.1429
11-69-27	0.1719	11-123-76	0.1391
12-69-28	0.1562	12-107-74	0.1233

12-69-27	0.1465	12-107-76	0.1213
13-85-28	0.1445	11-104-75	0.1137
13-85-27	0.1353	13-107-74	0.1123
13-34-57-31	0.0242	12-104-75	0.0883
12-104-75-31	0.0203	13-85-75	0.0866
13-85-76-31	0.0178	13-85-76	0.0724